remote sensing

MDPI

Article

Test of Determining Geopotential Difference between Two Sites at Wuhan Based on Optical Clocks' Frequency Comparisons

Anh The Hoang [1,2], Ziyu Shen [3,*], Kuangchao Wu [1], An Ning [1] and Wenbin Shen [1,4]

[1] Time and Frequency Geodesy Center, Department of Geophysics, School of Geodesy and Geomatics, Wuhan University, Wuhan 430079, China
[2] School of Agriculture and Natural Resource, Vinh University, Vinh City 460000, Vietnam
[3] School of Resource, Environmental Science and Engineering, Hubei University of Science and Technology, Xianning 437100, China
[4] State Key Laboratory of Information Engineering in Surveying, Mapping and Remote Sensing, Wuhan University, Wuhan 430079, China
* Correspondence: zyshen@hbust.edu.cn

Abstract: Applications of optical clocks in physical geodesy for determining geopotential are of increasing interest to scientists as the accuracy of optical clocks improves and the clock size becomes more and more compact. In this study, we propose a data processing method using the ensemble empirical mode decomposition technique to determine the geopotential difference between two sites in Wuhan based on the frequency comparison of two optical clocks. We use the frequency comparison record data of two Ca^+ optical clocks based on the optical fiber frequency transfer method, provided by the Innovation Academy for Precision Measurement Science and Technology, Chinese Academy of Sciences (Wuhan, China). By optical clock comparisons we obtained a geopotential difference of 42.50 ± 1.03 $m^2 \cdot s^{-2}$ (equivalent to height difference of 4.33 ± 0.11 m) between the two sites, which is excellent compared to the geopotential difference of 42.56 ± 0.29 $m^2 \cdot s^{-2}$ (equivalent to height difference of 4.34 ± 0.03 m) measured by a spirit leveling. The results show that the optical fiber frequency transfer method is promising in determining the geopotential and potential for unifying the world height system.

Keywords: OFFT; optical fiber; frequency transfer; geopotential; orthometric height

Citation: Hoang, A.T.; Shen, Z.; Wu, K.; Ning, A.; Shen, W. Test of Determining Geopotential Difference between Two Sites at Wuhan Based on Optical Clocks' Frequency Comparisons. *Remote Sens.* **2022**, *14*, 4850. https://doi.org/10.3390/rs14194850

Academic Editor: Alexander Braun

Received: 24 August 2022
Accepted: 24 September 2022
Published: 28 September 2022

1. Introduction

Based on Einstein's general relativity theory (GRT), clocks in positions with higher potentials run faster. Thus, when comparing the clock's frequencies at two points, we can determine the geopotential difference between those two points. Such applications of atomic clocks in geodesy are extensively investigated by scientists [1–5]. Studies show that to determine the geopotential difference with an accuracy of 0.1 $m^2 \cdot s^{-2}$ (equivalent to the orthometric height difference of 1 cm accuracy), we should determine the time shift or frequency shift at the accuracy level of about 1×10^{-18}.

With the development of clock technology, the accuracy of atomic clocks made significant improvements. Over the past decade, optical atomic clocks with frequency uncertainties of 10^{-18}, or even higher levels were consecutively generated [6–10], with the ability to sence a 7 mm variation in height [10]. In another aspect, the atomic clocks become more compact to be easily transported.

There are two ways to compare the frequencies between two remote clocks. The first one is transmitting frequency signals between two points via the GNSS satellite [11–17], which many scientists studied; for instance, the recently proposed tri-frequency combination approach (TFCA) [14]. The basic idea of the TFCA is to use three microwave links between a satellite and a ground station to determine the gravitational frequency shift and then the geopotential difference between them. Suppose the ground station emits a

frequency signal f_a, the satellite receives the signal, and then it immediately reflects the received signal f_b, and at the same time, the satellite emits a frequency signal f_c to the ground station. The geopotential difference between the ground station and the satellite is determined by combining the three frequencies based on the frequency shift equation [14]. If two ground stations simultaneously transmit and receive frequency signals with a common satellite, we can determine the geopotential difference between these two stations. The time-frequency system onboard the CSS (China Space Station) will be executed by the end of 2022, which will provide the potential test of determining the geopotential difference between two stations.

The second one is transmitting frequency signals between two points connected by optical fiber [18–27], simply referred to as the optical fiber frequency transfer (OFFT) method [28]. At present, the OFFT method holds the highest accuracy level because transmitting light signals via optical fiber can cancel out significant environmental noises. Recently, Takamoto et al. (2020) [27] used two transportable clocks to determine the geopotential difference and the height difference between two points in Tokyo Skytree, one at the tower's base and the other at the deck 450 m above, connected by optical fibers. The results show that the uncertainty based on OFFT using transportable optical clocks reached 5 cm and gravitational redshift measurements at the 10^{-5} level.

In this paper, focusing on applications of the OFFT approach in geodesy, we investigate the frequency comparison experiment of two optical clocks connected by optical fiber [26]. In Section 2, we present how to use the OFFT method to determine the geopotential difference. In Section 3, we present the frequency comparison experiment between two optical clocks. The data processing will be presented in Section 4. Results and discussions are provided in Sections 5 and 6 will draw the conclusions.

2. Method

The gravity frequency shift equation is the scientific basis for determining the geopotential difference between two points based on GTR. Suppose an optical clock at point A emits a frequency signal with f_A and a detector at point B receives the signal with f_B (Figure 1). Due to the difference in geopotential between these two points, f_A and f_B are different. We have the following equation [20,21,28]:

$$\frac{f_B - f_A}{f} = -\frac{W_B - W_A}{c^2} \tag{1}$$

where c is the speed of light in a vacuum; W_A and W_B are the geopotential at points A and B; Equation (1) is the gravity frequency shift equation, which describes the relationship between the frequency shift and the geopotential difference of two points according to GRT. If we can determine the frequency shift between the two clocks, noted as Δf_{AB} the geopotential difference ΔW_{AB} can be calculated as follows:

$$\Delta W_{AB} = W_B - W_A = -\frac{\Delta f_{AB}}{f} c^2 \tag{2}$$

If we use the spirit leveling method incorporating gravity data, we can also determine the geopotential difference value between two points A and B. When we compare this value with the value obtained from Equation (2), we can check the accuracy of the clock frequency comparison method. However, the determination of the orthometric height (OH) based on the OFFT method will not be possible if the position relative to the geoid of the clocks is not known. The general principle for determining the OH by the geopotential difference value is: in a height system that was chosen (for example, in China, the height reference point is the origin point at Qingdao), suppose we know the OH of point A and need to determine the OH of point B. From the OH of point A (known), we can determine the geopotential of point A. Based on the gravity frequency shift equation, the geopotential of point B can be determined. Then, based on the geopotential of point B, the OH of point

B can be determined (the gravity at point B could be measured). There are two special cases for using the OFFT method to determine the orthometric height. (1) If the two clocks are directly above each other so that the position of the geoid cancels [27]. (2) If the two clocks are sufficiently close together that there is negligible change in the position of the geoid between the two stations. In our experimental area there are no notable landform changes, and the straight distance between the two clocks is about 20 m. Hence, in this study, case 2 can be applied. Namely, at the present accuracy level, we may mention the height difference, which is equivalent to the corresponding geopotential difference.

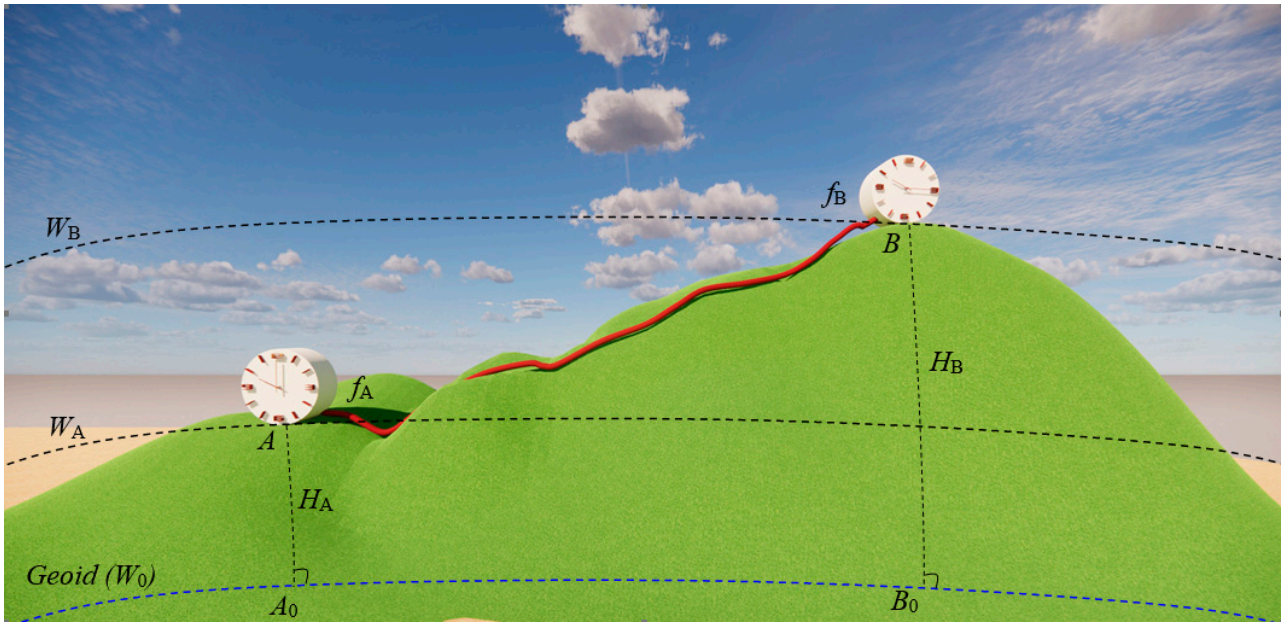

Figure 1. Determination of the geopotential difference by comparing optical clock frequency signals via optical fiber frequency transfer (OFFT) technique. The black dashed lines are equipotential surfaces passing through points A and B; the blue dashed line is the geoid. A_0 and B_0 are the intersection points of plumb lines passing through A, B, and the geoid, respectively; H_A and H_B are the orthometric heights of points A and B; W_A, W_B, and W_0 are geopotential at points A, B, and on the geoid, respectively; f_A is the frequency transmitted from an optical clock at point A, f_B is the frequency obtained by an optical clock at point B.

The principle of determining the orthometric height in this case is as follows:
The orthometric height of point A will be determined by the following equation [29]:

$$H_A = -\frac{W_A - W_0}{\overline{g}_A} \tag{3}$$

where $\overline{g}_A$ is a "mean value" of gravity along the plumb line; W_0 is the geopotential on the geoid, and we note that the W_0 value at present is a conventional value provided by the International Association of Geodesy (IAG). Since we cannot precisely determine the $\overline{g}_A$, in areas without major landform changes (plain region), $\overline{g}_A$ could be approximately replaced by $g_A + 0.0424H_A$ (where g_A is the surface gravity measurement, which can be measured by absolute gravimeter, in gal ($cm \cdot s^{-2}$)).

From Equation (3), suppose we know the orthometric height of point A, we can determine the geopotential of point A, expressed as:

$$W_A = W_0 - H_A(g_A + 0.0424H_A). \tag{4}$$

And geopotential of point B can be determined by the following equation:

$$W_B = W_A + \Delta W_{AB} = W_0 - H_A(g_A + 0.0424H_A) + \Delta W_{AB}. \quad (5)$$

Therefore, according to Equations (3) and (5), we can determine the orthometric height of point B, expressed as:

$$H_B = \frac{H_A(g_A + 0.0424H_A) - \Delta W_{AB}}{g_B + 0.0424H_B} \quad (6)$$

where the geopotential difference ΔW_{AB} is determined by Equation (2), in g.p.u (1 g.p.u = 1000 gal.m).

Equation (6) is an approximate formula, however, its accuracy is sufficient in the case of research points near the earth's surface. In this study area there are no notable landform changes.

Based on Equations (2) and (6), when we know the frequency shift Δf_{AB} between the two points A and B, so we can determine the orthometric height of point B.

3. Experiment Setup

The clocks used in the experiment are Ca^+ optical clocks with a systematic uncertainty of 1.3×10^{-17} (Figure 2a). At first, the two clocks were set at the same height for comparison. Then the two clocks were separated with a height difference of 4.34 ± 0.03 m measured by spirit leveling, which can be converted to the corresponding geopotential difference as 42.56 ± 0.29 $m^2 \cdot s^{-2}$ in our present case. The measurements were taken in January 2020 [26].

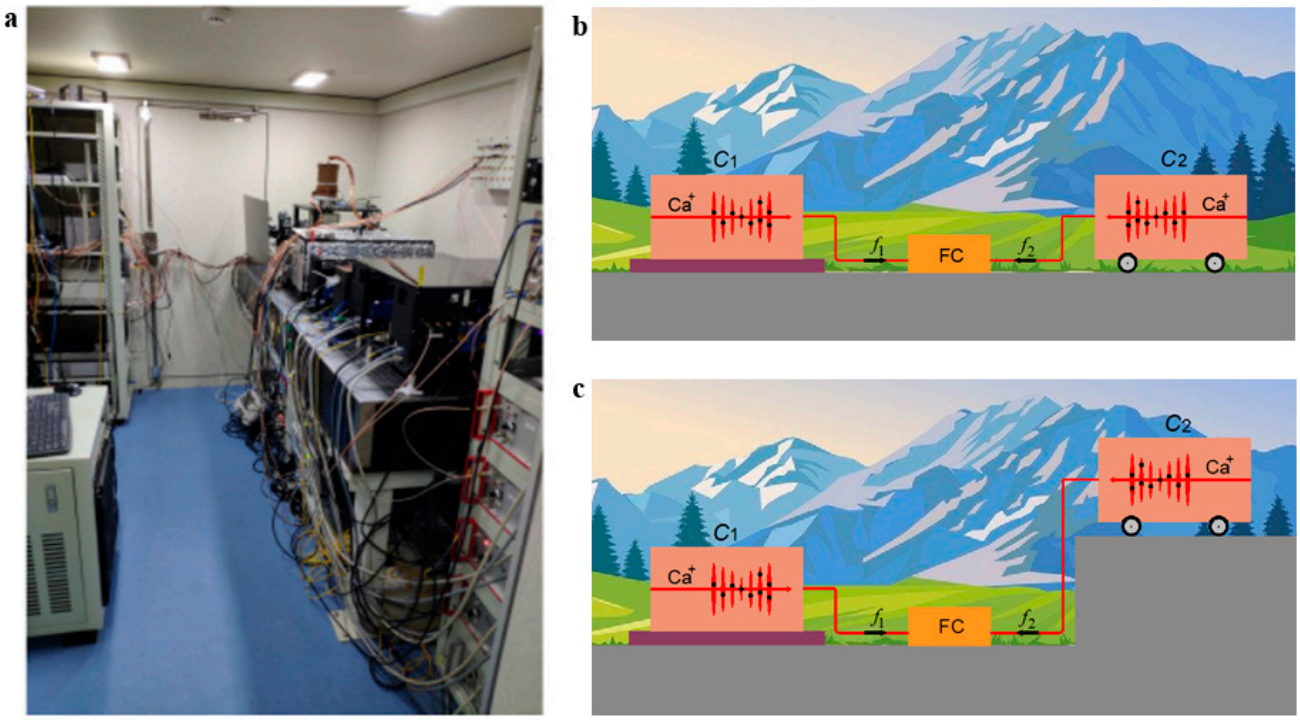

Figure 2. (**a**) Two Ca^+ optical clocks used located in the laboratory (courtesy of Huang et al., 2020 [26]). Scheme of experiment: (**b**) Ca^+ optical clocks C_1 and C_2 at same level in laboratory; (**c**) clock C_1 at laboratory level and C_2 at a height level above C_1 by 4.34 m.

The transportable optical clock is put into an air-conditioned car trailer with interior dimensions of $4.82 \times 2.3 \times 1.95$ m^3 in Wuhan. Huang and his colleagues compared the laboratory clock to the transportable clock Ca^+ (Figure 2b). Data obtained through comparison shows the frequency shift of the two clocks at the same height. Comparing

two clocks at the same height position helps us eliminate systematic errors in the data processing process. In addition to the frequency shift caused by gravitational potential differences, there is also the frequency shift caused by errors or systematic uncertainty. The transportable Ca^+ optical clock was moved 4.34 m higher than the old position, and the two clocks were connected by a 100 m-long noise canceled fiber, with straight distance being about 20 m (Figure 2c). By comparison, one obtains the frequency shifts between the two clocks at two different sites.

4. Data Processing

In this study, we used the datasets provided by Huang et al. (2020) [26]. One dataset covers 15 days when the two clocks have the same altitude, and the other covers 27 days when the two clocks have an altitude difference of 4.34 m (corresponding to a geopotential difference of 42.56 $m^2 \cdot s^{-2}$).

Because the original data contain many gross errors, we will first proceed to remove the anomalous large errors. The data obtained after this step will be included in the second processing step, which is noise removal. Here, we apply the ensemble empirical mode decomposition (EEMD) [30,31] for data processing. Various studies [16,17] demonstrated that the EEMD method is effective for processing different kinds of observations in a time series.

The original data are shown in Figure 3a and Figure 4a. To remove gross errors, we calculated the mean (M) and root mean square (RMS, σ) of the measurements for each day. Based on M and σ, from the original data, we deleted the anomalous value, namely the absolute value, the difference being that the mean M is more significant than $|2\sigma|$, then we obtained the residual sequence r_1, from which we calculated the new M_1 and σ_1. Repeating the above procedures, we obtained convergent sequences r_i, M_i, and σ_i ($i = 1, 2, \ldots N$) for further usage (see Figures 3b and 4b). For convenience, here we denote the data series after removing the gross errors as the residual time series $s(t)$. The correlation between the original data and the data after removing the gross errors are shown in Figure 5.

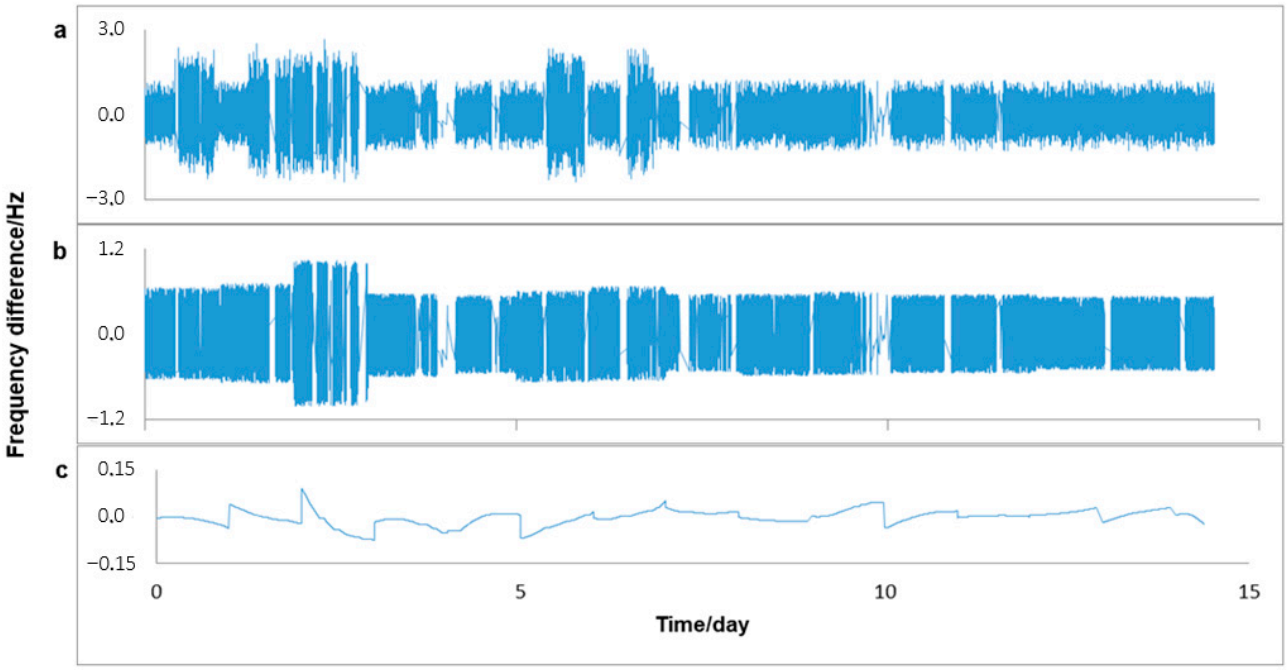

Figure 3. The frequency difference measurement between two optical clocks located at the same site. (**a**) Original data; (**b**) residual data after data processing, namely the gross errors removed; and (**c**) residual data after EEMD.

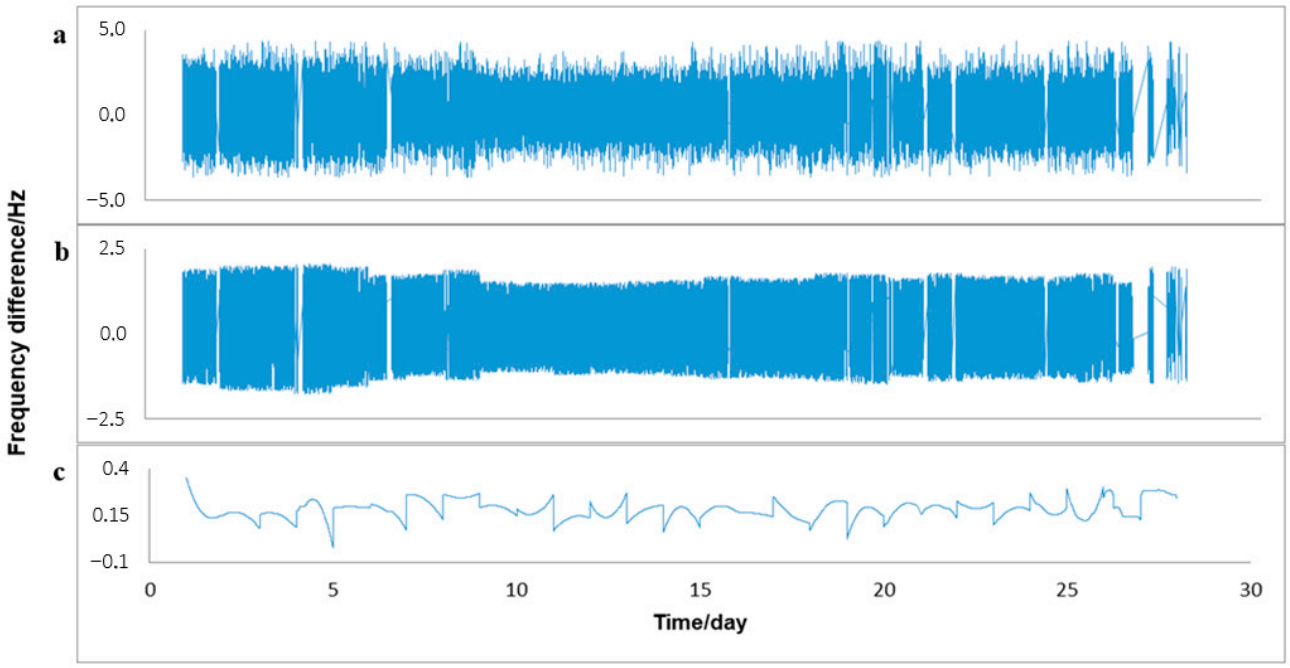

Figure 4. The measurement of the frequency difference between two optical clocks located at two sites with a height difference of 4.34m. (**a**) Original data; (**b**) after data processing, namely the gross errors being removed; and (**c**) residual data after EEMD.

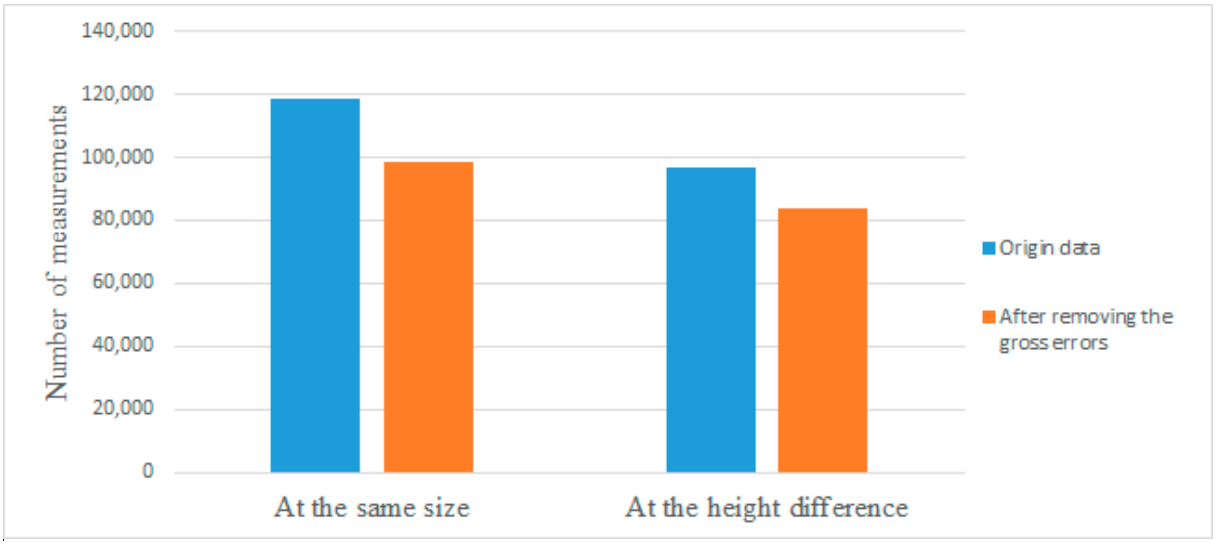

Figure 5. Correlation histogram of the original data and the data obtained after removing the gross errors.

To further remove the noises from the residual time series $s(t)$, we applied the EEMD technique [30,31] to the series $s(t)$. The steps to implement the EEMD method are stated as follows [30,31]:

(i) Using the data obtained $s(t)$, add the Gaussian white noise $n(t)$ to obtain a new signal data: $x(t) = s(t) + n(t)$. The addition of Gaussian white noise to the decomposition algorithm aims to stabilize the method's performance. The Gaussian white noise series has zero mean, so it will not affect the original signal and provide a uniform reference frame in the time frequency space. The added noise collates the portion of the signal of comparable scale in one intrinsic mode function (IMF) [30]. Therefore, the IMF mean values will maintain their

natural properties and are less affected by mode mixing. It is an improvement of the EEMD method over the empirical mode decomposition (EMD) method.

(ii) To process the new signal $x(t)$, identify all the local maxima points—$L\max(t)$ and local minima points—$L\min(t)$, and connect all these local maxima (minima) with a cubic spline as the upper (lower) envelope.

(iii) Caculate the local mean $m(t)$ of the two envelopes:

$$m(t) = \frac{L\max(t) + L\min(t)}{2}. \tag{7}$$

(iv) Caculate the first component $h(t)$ by taking the difference between the data $x(t)$ and the local mean $m(t)$:

$$h(t) = x(t) - m(t). \tag{8}$$

(v) Repeat steps (ii), (iii), and (iv) many times until $h(t)$ meets the under certain criteria of IMF. The final $h(t)$ is designated as $c_j(t)$ in the decomposition result. Thus, $x(t)$ is decomposed into a series of IMFs:

$$x(t) = \sum_{j=1}^{n} c_{\mathrm{j}} + r_{\mathrm{n}} \tag{9}$$

where c_{j} is components of the IMF, r_{n} is the residue of data $x(t)$.

(vi) Repeat steps (i) to (v) many times but with different Gaussian white noise each time.

(vii) Obtain the (ensemble) different c_{i} and a residual trend r as the final result.

This way, we obtain residual series $x(t)$ (see Figures 3c and 4c).

We use the residual series $x(t)$ to calculate the mean (M) and RMS (σ) for each day. Then, we calculate the weighted mean (Δf) and its RMS ($m_{\Delta f}$). The accuracy of the estimated weighted mean was calculated using the following formula [32,33]:

$$m_{\Delta f} = \sqrt{\frac{\sum_{i=1}^{n} P_i v_i v_i}{(n-1)\sum_{i=1}^{n} P_i}} \tag{10}$$

where $v_i = \Delta f_{\mathrm{i}} - \Delta f$ and $P_i = \frac{0.01}{\sigma_i^2}$.

Figures 3 and 4 show the frequency difference measurements of two clocks at the same location and two sites with an altitude difference of 4.34 m, respectively. As shown by Figures 3a and 4a, since the original data contain gross errors, the first step we take is removing the gross errors to obtain the preprocessed data. After data preprocessing, the frequency difference series become more stable, as shown in Figures 3b and 4b. All operations are based on the preprocessed data sets in the following data processing.

Then, the EEMD technique is applied to the preprocessed data sets for removing the periodic noises. Two preprocessed data at the two experimental locations (at the same location and two sites with the height difference) are decomposed into a series of intrinsic mode functions (IMF) and long trend components, as shown in Figures 6 and 7. From Figures 6 and 7, we can see that the periodic signals included in the data series are successfully identified (e.g., IMF10 (C10) in Figure 6 and IMF10 (C10) in Figure 7). The effectiveness of noise removal is shown in Figure 8, with a better trend change in the STD value across the processing steps of the EEMD method.

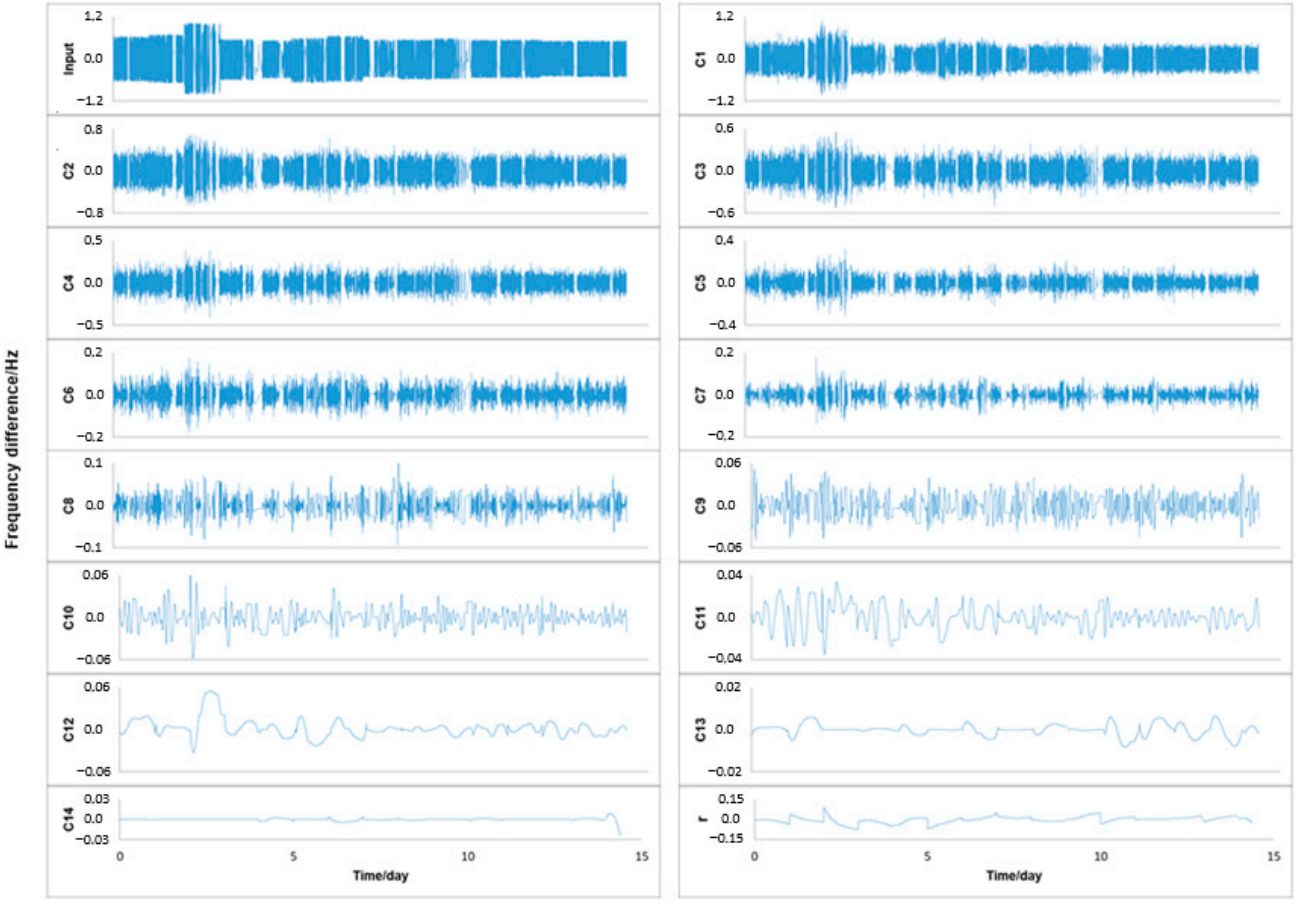

Figure 6. EEMD processing of the residual data series of the frequency difference between two optical clocks located at the same site. The input data (the **first panel**), its intrinsic mode functions (**C1**)–(**C14**), and the trend of (**r**).

In the EEMD processing, the periodic noises included in the preprocessed data were removed, and we reconstructed a new signal series by summing the residual components, denoted as r(t). The signal series r(t) is regarded as the geopotential-related signals. Then, based on it, we can determine the gravitational frequency shift value between two clocks. The signal series r(t) is considered as the EEMD results, as shown in Figures 3c and 4c. Compared to the original data, the results improved since the periodic noises were removed. The results in Figures 3 and 4 show that the processed data are more stable, the range of variation between the frequency values is no longer large, and the values converge asymptotic to the true value.

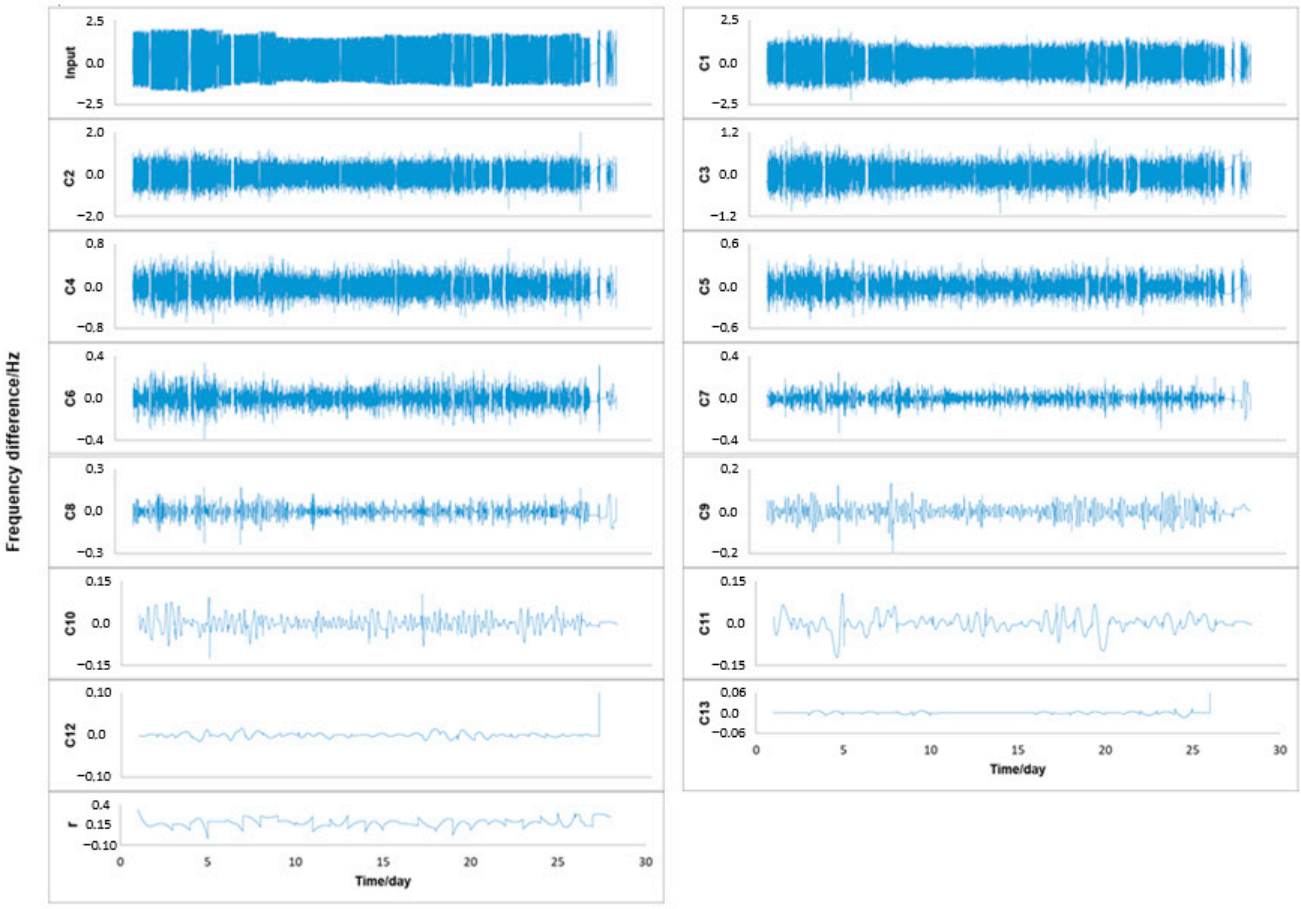

Figure 7. EEMD processing of the residual data series of the frequency difference between two optical clocks located at two sites with a height difference. The input data (the **first panel**), its intrinsic mode functions (**C1**)–(**C13**), and the trend of (**r**).

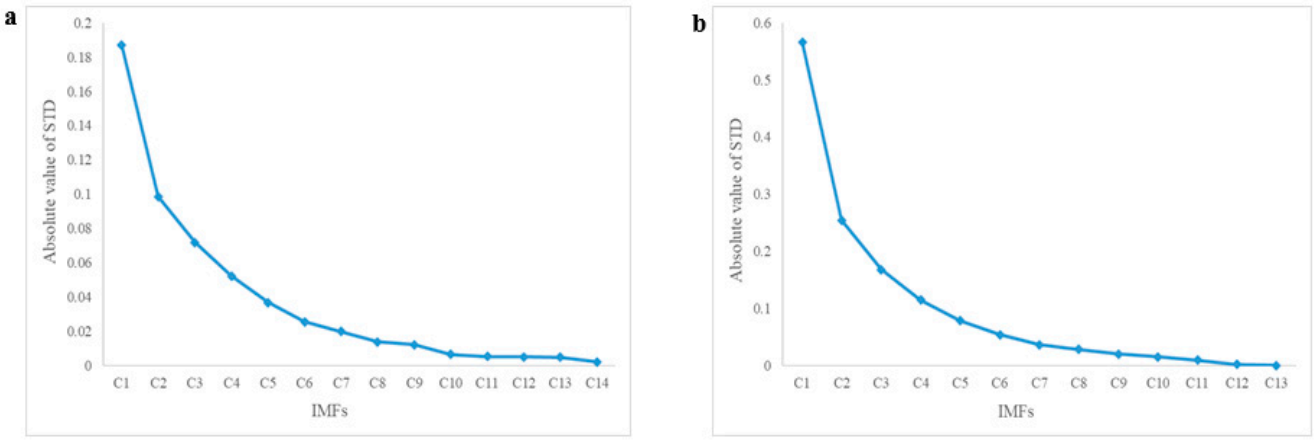

Figure 8. The change in the STD value of the data during EEMD processing. (**a**) at the same site; (**b**) at two different sites.

5. Results

Using the results obtained from the EEMD processing, we calculated the mean (M) and RMS (σ) of each day, and then calculate the weighted mean (Δf) and its RMS ($m_{\Delta f}$) according to Section 4. The stability of the measurement of the frequency difference between two clocks is described by Allan deviations [34–36] in Figure 9. The frequency noise is shown as black dashes and the blue dots are measurements. Figure 9a shows

the two clocks at the same site, with the average sampling cycle being 12 s, achieving a stability of $2.49 \times 10^{-17}/6$ d. Figure 9b shows two clocks at different sites, with the average sampling cycle being 25 s, achieving a stability of $1.45 \times 10^{-17}/12$ d. At the same site, the weighted mean is Δf_0 = (0.000924 ± 0.002005) Hz. Moreover, at two different sites with a height difference, the weighted mean is Δf_H = (0.195288 ± 0.004252) Hz. From the measurement results, the difference of frequency shift of the two clocks located at two different sites is 0.195288 − 0.000924 = 0.194364 Hz. With the clock frequency 411,042,129,776,400.41 Hz [26], c = 299,792,458 m/s, g = 9.80665 $m \cdot s^{-2}$, we obtained the geopotential difference 42.50 ± 1.03 $m^2 \cdot s^{-2}$ and the height difference of 4.33 ± 0.11 m (see Table 1). Compared to the height difference of 4.34 ± 0.03 m measured by spirit leveling (corresponding to a geopotential difference of 42.56 ± 0.29 $m^2 \cdot s^{-2}$), the result given here is better than the previous result of 4.22 ± 0.33 m [26]. This difference in results may come from the difference of data processing methods between this study and the previous study by Huang et al. (2020) [26]. First, by removing the raw errors, we obtain a more reliable data series before putting it into EEMD processing. Next, the EEMD method shows a very good noise filtering effect to obtain a convergent residual series with less noise. The results are shown in Figures 9–11 and Table 1.

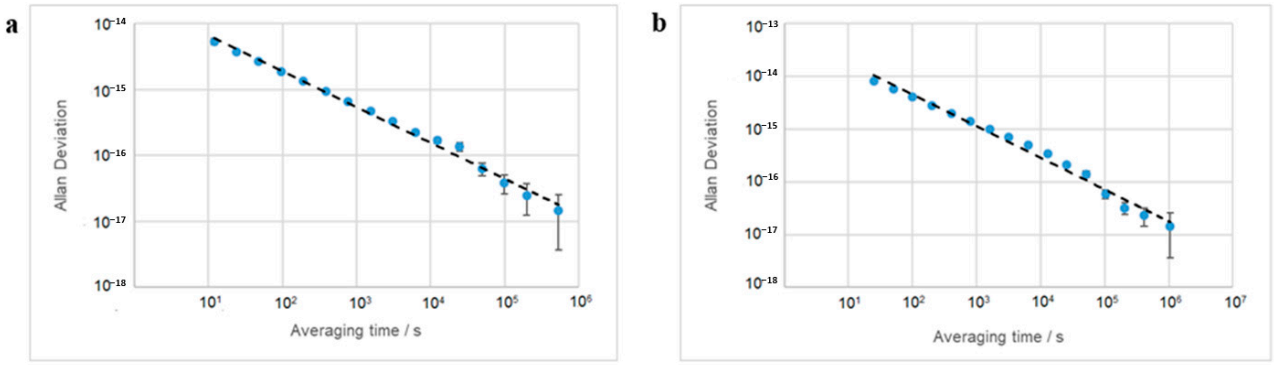

Figure 9. The Allan deviation of the frequency comparison series between two clocks. (**a**) at the same site; (**b**) at two different sites.

Table 1. Results of the height difference by frequency comparison.

Frequency Used Being (Hz)	Gravity Frequency Shift after Calibration (Hz)	*g* ($m \cdot s^{-2}$)	Geopotential Difference ($m^2 \cdot s^{-2}$)	Height Difference (m)
411,042,129,776,400.41	0.194364	9.80665	42.50 ± 1.03	4.33 (11)

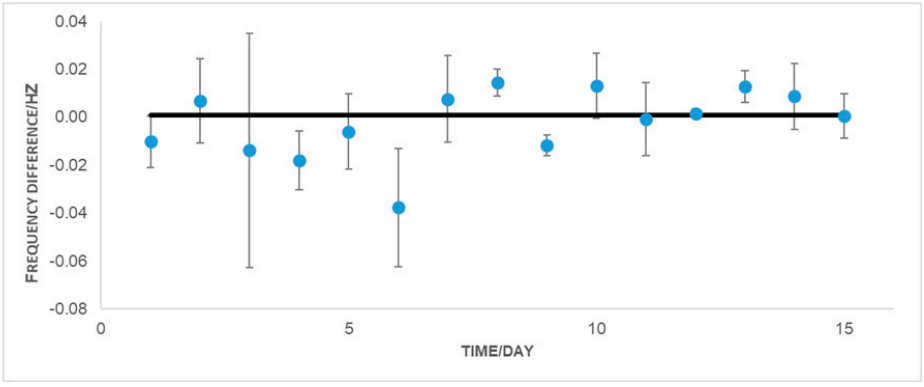

Figure 10. The mean of the frequency difference between two optical clocks located at the same site. Each blue point shows the frequency difference mean value between two optical clocks in one day, and gray vertical lines are the statistical uncertainty. The black horizontal line is the weighted mean.

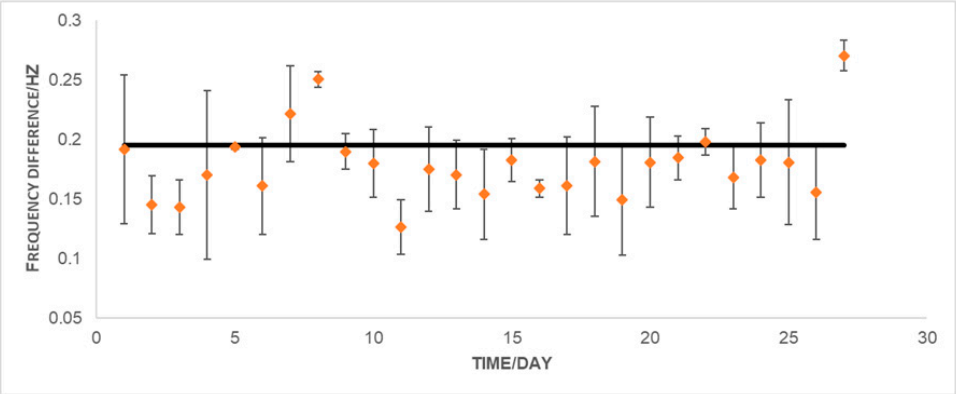

Figure 11. The mean of the frequency difference between two optical clocks located at two sites. Each orange point shows the frequency difference mean value between two optical clocks in one day, and gray vertical lines are the statistical uncertainty. The black horizontal line is the weighted mean.

6. Conclusions

In this study, we used the OFFT method to determine the geopotential difference between two points on the ground. First, we compared the frequencies of two clocks in the same laboratory via optical fibers. Then we transported one of the two clocks to a nearby site with a higher position and compared the frequency difference between these two clocks connected via optical fibers [26]. In this way, we determined the geopotential difference between these two sites.

The results in this study are consistent with the stability of the transportable Ca^+ clocks. We use the ensemble empirical mode decomposition (EEMD) technique to handle the residual data series. The results show that the EEMD method effectively filters out the noises of frequency transmission data over optical fiber. The frequency signals are usually nonlinear continuous signals and are affected quite a bit by noises. Processing these signals according to old transforms (short-time Fourier transform, wavelet transform, etc.) often does not yield the desired results. From the published studies [16,17,37] and the calculation results in this study, it is shown that the EEMD method is a suitable noise reduction method, which can be used to process frequency signals in geodetic measurements.

Huang et al. (2020) [26] performed the experiments as described in this study and obtained the results of 4.22 (33) m. In addition, they further performed frequency comparison experiments between the two Ca^+ clocks located at Wuhan and Beijing by GNSS time and the frequency transfer technique [16]. The results show that the height difference measured by the GNSS time frequency comparison technique [38,39] achieved only an accuracy level of tens of meters [26], which could be due to a severe impact of GNSS time and frequency transfer techniques. The frequency comparison results of the optical fiber frequency transfer (OFFT) method as presented in this study are much better than the previous study [26].

This study shows that the OFFT method is promising for determining the geopotential difference between two points on the ground. However, the limitation of this method is that there must be a fiber-optic connection between two remote points. To solve this problem, a new method currently being studied by scientists is to compare clocks by transmitting frequencies in free space, and the obtained experimental results are very positive [40,41]. Although at present, the optical fiber system is used extensively for various purposes, such as television and the internet, the use of the optical fiber system for geodesy purposes (specifically connecting two optical clocks) is a technique that needs to be studied further. In another aspect, flexibly transportable optical clocks are needed for extensive field applications. With the rapid development of time and frequency science, we expect an exciting future where compact and precise optical clocks will be extensively used to determine geopotential and unify the world height system at the centimeter level.

Author Contributions: Initiation and data collection, W.S.; methodology, A.T.H. and Z.S.; software, A.T.H.; data processing, A.T.H.; validation, A.T.H., A.N. and K.W.; formal analysis, A.T.H., Z.S. and W.S.; investigation, A.T.H. and Z.S.; original draft preparation, A.T.H.; writing—review and editing, A.T.H., Z.S., W.S., K.W. and A.N.; visualization, A.T.H.; supervision, Z.S. and W.S.; project administration, W.S. All authors have read and agreed to the published version of the manuscript.

Funding: This study is supported by the National Natural Science Foundation of China (NSFC) (Grant Nos. 41721003, 42030105, 41631072, 41874023, 41804012, 41974034), and Space Station Project (Grant No. 2020-228).

Institutional Review Board Statement: Not applicable.

Data Availability Statement: The data obtained in the study are available from the corresponding author upon reasonable request.

Acknowledgments: We would like to thank K. Gao and Y. Huang for sharing the data used in this study. We appreciate three anonymous reviewers for their valuable comments and suggestions, which greatly improved the manuscript.

Conflicts of Interest: The authors declare no conflict of interest.

References

1. Briatore, L.; Leschiutta, S. Evidence for the Earth gravitational shift by direct atomic-time-scale comparison. *Nuovo Cim. B* **1977**, *37*, 219–231. [CrossRef]
2. Ray, J.; Senio, K. Geodetic techniques for time and frequency comparisons using GPS phase and code measurements. *Metrologia* **2005**, *42*, 215–232. [CrossRef]
3. Shen, Z.Y.; Shen, W.B. Geopotential difference determination using optic-atomic clocks via coaxial cable time transfer technique and a synthetic test. *Geod. Geodyn.* **2015**, *6*, 344–350. [CrossRef]
4. Mai, E. *Time, Atomic Clocks, and Relativistic Geodesy*; Deutsche Geodätische Kommission, Reihe A, Theoretische Geodäsie, Heft Nr. 124, Verlag der Bayerischen Akademie der Wissenschaften: München, Germany, 2013.
5. Flury, J. Relativistic geodesy. *J. Phys. Conf. Ser.* **2016**, *723*, 012051. [CrossRef]
6. Hinkley, N.; Sherman, J.A.; Phillips, N.B.; Schioppo, M.; Lemke, N.D.; Beloy, K.; Pizzocaro, M.; Oates, C.W.; Ludlow, A.D. An atomic clock with 10^{-18} instability. *Science* **2013**, *341*, 1215–1218. [CrossRef]
7. Nicholson, T.L.; Campbell, S.L.; Hutson, R.B.; Marti, G.E.; Bloom, B.J.; McNally, R.L.; Zhang, W.; Barrett, M.D.; Safronova, M.S.; Strouse, G.F.; et al. Systematic evaluation of an atomic clock at 2×10^{-18} total uncertainty. *Nat. Commun.* **2015**, *6*, 6896. [CrossRef] [PubMed]
8. Ushijima, I.; Takamoto, M.; Das, M.; Ohkubo, T.; Katori, H. Cryogenic optical lattice clocks. *Nat. Photonics* **2015**, *9*, 185–189. [CrossRef]
9. Huntemann, N.; Sanner, C.; Lipphardt, B.; Tamm, C.; Peik, E. Single-ion atomic clock with 3×10^{-18} systematic uncertainty. *Phys. Rev. Lett.* **2016**, *116*, 063001. [CrossRef]
10. Oelker, E.; Hutson, R.; Kennedy, C.; Sonderhouse, L.; Bothwell, T.; Goban, A.; Kedar, D.; Sanner, C.; Robinson, J.M.; Marti, G.E.; et al. Demonstration of 4.8×10^{-17} stability at 1 s for two independent optical clocks. *Nat. Photonics* **2019**, *13*, 714–719. [CrossRef]
11. Shen, W.B.; Ning, J.S. The application of GPS technique in determining the Earth's potential field. *J. Glob. Position. Syst.* **2005**, *4*, 268–276. [CrossRef]
12. Delva, P.; Hees, A.; Bertone, S.; Richard, E.; Wolf, P. Test of the gravitational redshift with stable clocks in eccentric orbits: Application to Galileo satellites 5 and 6. *Class. Quantum Gravity* **2015**, *32*, 232003. [CrossRef]
13. Shen, Z.Y.; Shen, W.B.; Zhang, S.X. Formulation of geopotential difference determination using optical-atomic clocks onboard satellites and on ground based on Doppler cancellation system. *Geophys. J. Int.* **2016**, *206*, 1162–1168. [CrossRef]
14. Shen, Z.Y.; Shen, W.B.; Zhang, S.X. Determination of gravitational potential at ground using optical-atomic clocks on board satellites and on ground stations and relevant simulation experiments. *Surv. Geophys.* **2017**, *38*, 757–780. [CrossRef]
15. Shen, W.B.; Sun, X.; Cai, C.H.; Wu, K.C.; Shen, Z.Y. Geopotential determination based on a direct clock comparison using two-way satellite time and frequency transfer. *Terr. Atmos. Ocean. Sci.* **2019**, *30*, 21–31. [CrossRef]
16. Shen, W.B.; Wu, K.C.; Sun, X.; Cai, C.H.; Shen, Z.Y. Preliminary experimental results of determining the geopotential difference between two synchronized portable hydrogen clocks at different locations. *arXiv* **2020**, arXiv:2008.06271. [CrossRef]
17. Wu, K.C.; Shen, Z.Y.; Shen, W.B.; Sun, X.; Cai, C.H.; Wu, Y.F. A preliminary experiment of determining the geopotential difference using two hydrogen atomic clocks and TWSTFT technique. *J. Geod. Geodyn.* **2020**, *11*, 229–241. [CrossRef]
18. Śliwczyński, Ł.; Krehlik, P.; Czubla, A.; Buczek, Ł.; Lipiński, M. Dissemination of time and RF frequency via a stabilized fibre optic link over a distance of 420 km. *Metrologia* **2013**, *50*, 133–145. [CrossRef]

19. Predehl, K.; Grosche, G.; Raupach, S.M.F.; Droste, S.; Terra, O.; Alnis, J.; Legero, T.; Hänsch, T.W.; Udem, T.; Holzwarth, R.; et al. A 920-kilometer optical fiber link for frequency metrology at the 19th decimal place. *Science* **2012**, *336*, 441–444. [CrossRef] [PubMed]
20. Shen, W.B. Orthometric height determination based upon optical clocks and fiber frequency transfer technique. In Proceedings of the Saudi International Electronics, Communications and Photonics Conference, Riyadh, Saudi Arabia, 27–30 April 2013; pp. 1–4.
21. Shen, W.B. Orthometric height determination using optical clocks. In Proceedings of the EGU General Assembly Conference Abstracts, Vienna, Austria, 7–12 April 2013; p. 5214.
22. Takano, T.; Takamoto, M.; Ushijima, I.; Ohmae, N.; Akatsuka, T.; Yamaguchi, A.; Kuroishi, Y.; Munekane, H.; Miyahara, B.; Katori, H. Geopotential measurements with synchronously linked optical lattice clocks. *Nat. Photonics* **2016**, *10*, 662–666. [CrossRef]
23. Lisdat, C.; Grosche, G.; Quintin, N.; Shi, C.; Raupach, S.; Grebing, C.; Nicolodi, D.; Stefani, F.; Al-Masoudi, A.; Dörscher, S.; et al. A clock network for geodesy and fundamental science. *Nat. Commun.* **2016**, *7*, 12443. [CrossRef] [PubMed]
24. Grotti, J.; Koller, S.; Vogt, S.; Häfner, S.; Sterr, U.; Lisdat, C.; Denker, H.; Voigt, C.; Timmen, L.; Rolland, A.; et al. Geodesy and metrology with a transportable optical clock. *Nat. Phys.* **2018**, *14*, 437–441. [CrossRef]
25. Shen, Z.Y.; Shen, W.B.; Peng, Z.; Liu, T.; Zhang, S.G.; Chao, D.B. Formulation of determining the gravity potential difference using ultra-high precise clocks via optical fiber frequency transfer technique. *J. Earth Sci.* **2019**, *30*, 422–428. [CrossRef]
26. Huang, Y.; Zhang, H.Q.; Zhang, B.L.; Hao, Y.M.; Guan, H.; Zeng, M.Y.; Chen, Q.F.; Lin, Y.G.; Wang, Y.Z.; Cao, S.Y.; et al. Geopotential measurement with a robust, transportable Ca^{+} optical clock. *Phys. Rev. A* **2020**, *102*, 050802. [CrossRef]
27. Takamoto, M.; Ushijima, I.; Ohmae, N.; Yahagi, T.; Kokado, K.; Shinkai, H.; Katori, H. Test of general relativity by a pair of transportable optical lattice clocks. *Nat. Photonics* **2020**, *14*, 411–415. [CrossRef]
28. Hoang, A.T.; Shen, Z.Y.; Shen, W.B.; Cai, C.H.; Xu, W.; Ning, A.; Wu, Y.F. Determination of the orthometric height difference based on optical fiber frequency transfer technique. *J. Geod. Geodyn.* **2021**, *12*, 405–412. [CrossRef]
29. Hofmann-Wellenhof, B.; Moritz, H. *Physical Geodesy*; Springer: Vienna, Austria, 2005.
30. Wu, Z.H.; Huang, N.E. Ensemble empirical mode decomposition: A noise-assisted data analysis method. *Adv. Adapt. Data Anal.* **2009**, *1*, 1–41. [CrossRef]
31. Huang, N.E.; Wu, Z.H. A review on Hilbert-Huang transform: Method and its applications to geophysical studies. *Rev. Geophys.* **2008**, *46*, RG2006. [CrossRef]
32. Reichmann, W.J. *Use and Abuse of Statistics*; Methuen Co. Ltd.: London, UK, 1961; Reprinted 1964–1970 by Pelican Appendix 8.
33. Hassani, H.; Ghodsi, M.; Howell, G. A note on standard deviation and standard error. *Teach. Math. Its Appl. Int. J. IMA* **2010**, *29*, 108–112. [CrossRef]
34. Allan, D.W. Statistics of atomic frequency standards. *Proc. IEEE* **1966**, *54*, 221–230. [CrossRef]
35. Allan, D.W. Time and frequency (Time-Domain) characterization, estimation, and prediction of precision clocks and oscillators. *IEEE Trans. Ultrason. Ferroelectr. Freq. Control* **1987**, *34*, 647–654. [CrossRef]
36. Banerjee, P.; Chatterjee, A.; Suman, A. Determination of Allan deviation of Cesium atomic clock for lower averaging time. *Indian J. Pure Appl. Phys.* **2007**, *45*, 945–949.
37. Gasi, S. A new ensemble empirical mode decomposition (EEMD) denoising method for seismic signals. *Energy Procedia* **2016**, *97*, 84–91. [CrossRef]
38. Cai, C.H.; Shen, W.B.; Shen, Z.Y.; Xu, W. Geopotential determination based on precise point positioning time comparison: A case study using simulated observation. *IEEE Access.* **2020**, *8*, 204283–204294. [CrossRef]
39. Xu, W.; Shen, W.B.; Cai, C.H.; Li, L.H.; Wang, L.; Shen, Z.Y. Modeling and performance evaluation of precise positioning and time-frequency transfer with Galileo five-frequency observations. *Remote Sens.* **2021**, *13*, 2972. [CrossRef]
40. Dix-Matthews, B.P.; Schediwy, S.W.; Gozzard, D.R.; Savalle, E.; Esnault, F.-X.; Lévèque, T.; Gravestock, C.; D'Mello, D.; Karpathakis, S.; Tobar, M.; et al. Point-to-point stabilized optical frequency transfer with active optics. *Nat. Commun.* **2021**, *12*, 515. [CrossRef]
41. Bodine, M.I.; Deschênes, J.-D.; Khader, I.H.; Swann, W.C.; Leopardi, H.; Beloy, K.; Bothwell, T.; Brewer, S.M.; Bromley, S.L.; Chen, J.-S.; et al. Optical atomic clock comparison through turbulent air. *Phys. Rev. Res.* **2020**, *2*, 033395. [CrossRef]